Scripta Materialia 187 (2020) 202–209

Contents lists available at ScienceDirect

Scripta Materialia

journal homepage: www.elsevier.com/locate/scriptamat

Viewpoint set

Promising properties and future trend of eutectic high entropy alloys

Yiping Lu[a,*], Yong Dong[b], Hui Jiang[c], Zhijun Wang[d,*], Zhiqiang Cao[a], Sheng Guo[e,*], Tongmin Wang[a], Tingju Li[a], Peter K. Liaw[f]

[a] Key Laboratory of Solidification Control and Digital Preparation Technology (Liaoning Province), School of Materials Science and Engineering, Dalian University of Technology, Dalian 116024, China
[b] School of Materials and Energy, Guangdong University of Technology, Guangzhou 510006, China
[c] College of Mechanical and Electronic Engineering, Shandong University of Science and Technology, Qingdao 266590, China
[d] State Key Laboratory of Solidification Processing, Northwestern Polytechnical University, Xi'an 710072, China
[e] Industrial and Materials Science, Chalmers University of Technology, SE-41296 Gothenburg, Sweden
[f] Department of Materials Science and Engineering, The University of Tennessee, Knoxville, TN 37996, USA

ARTICLE INFO

Article history:
Received 26 February 2020
Revised 6 June 2020
Accepted 6 June 2020
Available online 18 June 2020

Keywords:
Eutectic alloys
High-entropy alloys
Castability
Microstructure
Mechanical properties

ABSTRACT

Eutectic high-entropy alloys (EHEAs), as a sub-group of high-entropy alloys (HEAs), are becoming a new research hotspot in the metallic materials community because of their excellent castability, fine and uniform microstructures even in the as-cast state, high strength, and good ductility. Some of the EHEAs have shown promising potentials for industrial applications. Here, the history, interesting solidification microstructure and mechanical properties, and the design strategy of EHEAs are reviewed, and their future prospects are outlined.

1. Introduction

Since 2004, a new type of alloys, high entropy alloys (HEAs) or multi-principal-element alloys, proposed by Yeh and Cantor et al. [1,2], have become a new research frontier in the metallic materials community [3–8]. Compared with the conventional metallic alloys based on one or two principal elements, HEAs generally contain at least four principal elements. The concept of HEAs is a breakthrough to the alloy design in the traditional physical metallurgy and opens a new field for explorations of new materials with novel properties. Nevertheless, most HEAs do not show superior mechanical properties, relative to those of conventional alloys if they are in the form of simple solid solutions, which are stabilized by the high mixing entropy in HEAs. Not surprisingly, researchers in the HEAs community turned to develop multi-phase HEAs to improve their mechanical properties but that generally would lead to the problem of poor castability. In fact, casting of HEAs, particularly at a large scale (kilogram scale) is quite often a challenge, since most HEAs do not possess good castability and they exhibit considerable chemical inhomogeneity in directly cast alloys, which retard their industrial applications.

On the other hand, it is well known that eutectic alloys are the most widely used casting alloys in industries. Generally, the eutectic alloys have the following features: 1) near-equilibrium microstructures that resist changes at temperatures as high as their reaction temperatures; 2) low-energy phase boundaries; 3) controllable microstructures; 4) high rupture strength; 5) stable defect structures; 6) good high-temperature creep resistance; 7) regular lamellar or rod-like eutectic structures, forming an in-situ composite [9]. In addition, eutectic alloys are known to have good castability. Also importantly, since the eutectic reaction is an isothermal transformation without a solidification-temperature range, both the segregation and shrinkage cavity can be alleviated. From the mechanical properties perspective, it is already known that in general single-phased body-centered-cubic (bcc)-structured HEAs have limited ductility, while single-phased face-centered-cubic (fcc)-structured HEAs could have high ductility but their strength is low. How to reach the simultaneous high strength and high ductility is another challenge for the engineering application of HEAs. Accordingly, if eutectic HEAs (EHEAs) with the composite fcc/bcc structures can be prepared, they could possess the advantageous mechanical properties and castability, clearing obstacles for their technological applications. Many metallic parts of in-

* Corresponding authors.
E-mail addresses: luyiping@dlut.edu.cn, 82713860@qq.com (Y. Lu), zhjwang@nwpu.edu.cn (Z. Wang), sheng.guo@chalmers.se (S. Guo).

https://doi.org/10.1016/j.scriptamat.2020.06.022
1359-6462/

dustrial equipment are made by direct casting, such as propeller, generator housing, engine housing, and various metal ball valves, and adapters. If the casting quality is poor, it is impossible to eliminate the casting defects through thermomechanical treatments, especially for complex and large ingots. Therefore, the casting performance and mechanical properties of the as-cast alloys are very important for the industrial applications of engineering alloys.

To address the above-mentioned problems for the real applications of HEAs, Lu et al. [10,11] firstly proposed to use the eutectic-alloy concept to design HEAs, aiming at good castability of HEAs. They [10,11] also used the eutectic alloy idea to design HEAs with the composite structure, or it can be said to use the HEA concept to design eutectic alloys. Furthermore, they proposed to design the eutectic alloys with a mixture of soft fcc and hard bcc phases, to achieve the balance of the high fracture strength and great ductility. Since then, more and more researchers have been attracted by the advantages of EHEAs and their great potential in industrial applications, and have dedicated to the research on EHEAs [10,11].

At present, there are more than 100 papers on EHEAs. The first reported EHEAs is the $AlCoCrFeNi_{2.1}$ alloy, with the tensile fracture strength over 1000 MPa, good ductility and great seawater corrosion resistance. The corrosion resistance and strength of this $AlCoCrFeNi_{2.1}$ alloy exceed that of copper alloys used in all marine applications, and its density is lower than that of copper alloys [11]. Subsequently, many EHEAs with excellent mechanical properties and special functionality have been reported [12-21]. EHEAs generally exhibit fine and uniform regular lamellar microstructures with lamella widths ranging from a few microns to tens of nanometers [22]. Even in kilogram-scale casting ingots, it is possible to obtain ultrafine lamellar microstructures with a lamella width of ~ 100 nm by ordinary solidifications [23,24]. The ease of achieving ultrafine microstructures in directly cast alloys is rarely seen in traditional alloys, including traditional eutectic alloys, which is directly related to the compositional complexity and the resultant slower elemental diffusion and growth rate of EHEAs, compared to those in conventional alloys. Certainly, a more detailed and systematic study of solidification mechanism of EHEAs is still needed.

2. The solidification microstructures and properties of EHEA

Conventional eutectic alloy solidification is usually via the reaction of $L \rightarrow \alpha + \beta$ or $L \rightarrow \alpha + \beta + \gamma$, where L is the liquid phase, and α, β and γ are individual phases in binary eutectic or ternary eutectic alloys. A summary of the reported EHEAs with completely eutectic microstructure is given in Table 1 [10,12,17–19,22,25–50]. It can be seen that all reported EHEAs with completely eutectic microstructures consist of a two-phase structure, and three-phase EHEAs have not been reported yet, which is quite different from traditional eutectic alloys. This phenomenon could be due to the complicated solidification mechanism of EHEAs and the difficulty with diffusion and coupling, restricting the formation of ternary eutectic phases, which again indicates that the solidification mechanism of EHEAs needs to be further studied.

Most EHEAs display a lamellar structure, and a small portion of EHEAs show a cellular eutectic structure. The lamella of some EHEAs grow in a divergent manner to form eutectic cells. The outer edges of the lamella are thicker, while the inner lamella are thinner, as shown in Fig. 1 [22]. Such lamellar structures with the radial growth and thickening along the growth direction are common in EHEAs but are rare in conventional eutectic alloys. The solidification structure of EHEAs is generally fine, some with lamella widths ranging from one to several microns, and some even down to tens of nanometers to 100 nanometers, like that in Fig. 2 [49]. Jiang et al. reported an industrial-scale $CoCrFeNiNb_{0.45}$ EHEA cast ingot with the interlamellar spacing of ~ 100 nm using normal casting methods, as shown in Fig. 3 [23]. Such an ultrafine solidification structure is rarely seen in conventional eutectic alloys and has never been found in conventional eutectic alloys in bulk ingots. EHEAs generally have excellent structural stability. Jiang et al. reported that the lamellar structure of $CoCrFeNiNb_{0.45}$ EHEAs is stable as obvious spheroidization and significant coarsening were not observed when the temperature is kept at 600 – 1,000 °C for 4 h, as exhibited in Fig. 4 [23].

EHEAs composed of BCC/B2 and BCC/intermetallic phases are generally brittle and have no tensile plasticity, while some EHEAs composed of a soft and a hard phases, like FCC/BCC (or B2), show excellent mechanical properties. The prototype EHEA, $AlCoCrFeNi_{2.1}$, displays a tensile fracture strength of 1,000 MPa and an elongation around 15%. Later, it was [12,17-19] reported that some as-cast EHEAs also present excellent mechanical properties with the tensile fracture strength up to 1,200 MPa. Such a high strength in as-cast EHEAs is extremely rarely seen in conventional alloys.

3. The alloy design of EHEAs

Although many EHEAs have been identified, how to design EHEAs is still a great challenge. Till now, some design strategies using for example the mixing enthalpy [46], a simple mixing method [49], the calculation of phase diagram (CALPHAD) method, and grouping and machine learning [50,51] have been reported, and they are briefly summarized below.

3.1. The mixing enthalpy method

Lu et al. [46] firstly proposed to use the mixing enthalpy method to pinpoint new EHEA compositions based on known ones. Alloy elements are divided into two different atomic groups by the mixing enthalpy. For one group, the mixing enthalpy between elements is close to zero, while elements possess the negative mixing enthalpy in the other group. For example, in the $AlCoCrFeNi_{2.1}$ EHEA, one group contains Co, Cr, and Fe elements, and the other group contains Al and Ni elements. From this alloy, new eutectic alloys were designed by replacing one element in the group of elements possessing the very negative mixing enthalpy group by another element, called the mixing enthalpy method. Similar to Al, the four elements, Zr, Nb, Hf, and Ta, also possess a very negative mixing enthalpy with Ni ($\Delta H_{mix\ (Al\text{-}Ni)}$ = -22 kJ/mol, $\Delta H_{mix\ (Zr\text{-}Ni)}$ = -49 kJ/mol, $\Delta H_{mix\ (Nb\text{-}Ni)}$ = -30 kJ/mol, $\Delta H_{mix\ (Hf\text{-}Ni)}$ = -42 kJ/mol, $\Delta H_{mix\ (Ta\text{-}Ni)}$ = -29 kJ/mol). Therefore, one can use Zr, Nb, Hf, and Ta elements to replace the Al element in the $AlCoCrFeNi_{2.1}$ EHEA, forming M (M = Zr, Nb, Hf, Ta)$_x$$CoCrFeNi_{2.1}$ EHEAs. The required contents of Zr, Nb, Hf, and Ta elements to form EHEAs, and their corresponding mixing enthalpy with Ni shows a connection to the case in $AlCoCrFeNi_{2.1}$, as is described by the following equations:

$$\frac{Zr}{Al}=\frac{x}{1}=-\frac{22}{-49},\ x0.45;\ \frac{Nb}{Al}=\frac{x}{1}=-\frac{22}{-30},\ x0.73;\ \frac{Hf}{Al}=\frac{x}{1}=-\frac{22}{-42},\ x0.52;\ \frac{Ta}{Al}=\frac{x}{1}=-\frac{22}{-29},\ x0.76$$

Thus, a series of new EHEAs, $Zr_{0.6}CoCrFeNi_{2.0}$, $Nb_{0.74}CoCrFeNi_{2.0}$, $Hf_{0.55}CoCrFeNi_{2.0}$ and $Ta_{0.65}CoCrFeNi_{2.0}$, have been located after some minor compositional adjustments. Fig. 5 gives the microstructure of the designed EHEAs.

3.2. A simple mixing method

The simple mixing method by considering the mixing enthalpy and constituent binary eutectics was proposed by Jiang et al. [49]. Required elements in EHEAs can be easily identified according to

Table 1.
A collection of reported EHEAs with completely eutectic microstructure [10,12,17–19,22,25–50]

Nos	Alloys	Morphology	eutectic structure	References
1	$AlCoCrFeNi_{2.1}$	eutectic	(FeCoCr)-FCC + (AlNi)-B2	[10]
2	$Al_{1.2}CrCuFeNi_2$	eutectic	(FeCr)-FCC + [(NiCu)Al]CrFe)-B2	[25]
3	$Co_{30}Cr_{10}Fe_{10}Al_{18}Ni_{32}$	eutectic	FCC+BCC	[26]
4	$AlCrFeNi_3$	eutectic	(FeCrNi)-FCC + (AlNi)-B2	[12]
5	$AlCo_{0.2}CrFeNi_{2.8}$	eutectic	(FeCoCrNi)-FCC + (AlNi)-B2	[12]
6	$AlCo_{0.4}CrFeNi_{2.6}$	eutectic	(FeCoCrNi)-FCC + (AlNi)-B2	[12]
7	$AlCo_{0.6}CrFeNi_{2.4}$	eutectic	(FeCoCrNi)-FCC + (AlNi)-B2	[12]
8	$AlCo_{0.8}CrFeNi_{2.2}$	eutectic	(FeCoCrNi)-FCC + (AlNi)-B2	[12]
9	$CrFeNi_{2.2}Al_{0.8}$	eutectic	(FeCrNi)-FCC + (AlNi)-B2	[18]
10	$Al_{16}Co_{41}Cr_{15}Fe_{10}Ni_{18}$	eutectic	(FeCoCrNi)-FCC + (AlNi)-rich BCC	[27]
11	$Ni_{30}Co_{30}Cr_{10}Fe_{10}Al_{18}W_2$	eutectic	(FeCoCrNi)-FCC + (AlNi)-rich B2	[19]
12	$CoCrFeNiZr_{0.5}$	eutectic	(FeCoCr)-FCC+Zr-rich Laves	[28]
13	$CoCrFeNiTa_{0.395}$	eutectic	(FeCr)-FCC + Ta-rich Laves	[29]
14	$CoCrFeNiMnPd_{0.6}$	eutectic	(CoCrFeNiMn)-FCC + Mn_xPd_y	[30]
15	CoCrFeNiMnPd	eutectic	(CoCrFeNiMn)-FCC + Mn_xPd_y	[30]
16	$CoCrFeNiMnPd_{1.4}$	eutectic	(CoCrFeNiMn)-FCC + Mn_xPd_y	[30]
17	$CoCrFeNiMnPd_{1.8}$	eutectic	(CoCrFeNiMn)-FCC + Mn_xPd_y	[30]
18	$Co_{25}Fe_{25}Mn_5Ni_{25}Ti_{20}$	eutectic	(Fe,Co,Ni)-rich FCC+Ti_2(Ni,Co)	[31]
19	$CoFeNiNb_{0.5}$	eutectic	(Fe,Co,Ni)-rich FCC+Nb-rich Laves	[32]
20	$V_{10}Cr_{15}Mn_5Co_{10}Ni_{25}Fe_{25.3}Nb_{9.7}$	eutectic	(Fe,Cr)-rich FCC+Nb-rich Laves	[33]
21	AlCrFeNi	eutectic	(AlNi)-BCC1 + (FeCr)-BCC2	[22]
22	$AlCrFeNiMo_{0.2}$	eutectic	(AlNi)-BCC1 + (FeCrMo)-BCC2	[22]
23	$CoCrFeNiNb_{0.65}$	eutectic	(FeCrNi)-FCC + (CoNiNb)Laves	[34]
24	$Nb_{25}Sc_{25}Ti_{25}Zr_{25}$	eutectic	(Sc,Zr)-HCP + (TiZrNb)-BCC	[35]
25	$Ni_2FeCoV_{0.5}Nb_{0.75}$	eutectic	(FeNiV)-FCC + (CoNb)-Laves	[36]
26	$CoFeNiVMo_{0.6}$	eutectic	(FeCoNiV)-FCC + $CoMo_2NiV$-type IM	[37]
27	$CoFeNi_{1.4}VMo$	eutectic	(FeCoNi)FCC + Co_2Mo_3-type IM	[37]
28	$Co_2Mo_{0.8}Ni_2VW_{0.8}$	eutectic	(CoNiV)-FCC + (W,Mo,V)-μ	[38]
29	$Al_{19.3}Co_{15}Cr_{15}Ni_{50.7}$	eutectic	Al-poor FCC + Al-rich B2	[39]
30	$CoCrFeNiMo_{0.8}$	eutectic	FCC+$Cr_9Mo_{21}Ni_{20}$-type intermetallic	[40]
31	$Fe_{20}Co_{20}Ni_{41}Al_{19}$	eutectic	(Fe,Co)-rich $L1_2$+(AlNi)-B2	[17]
32	$Al_{1.3}CrFeNi$	eutectic	(Fe,Cr)-BCC+(AlNi)-B2	[41]
33	$Fe_{28.2}Ni_{18.8}Mn_{32.9}Al_{14.1}Cr_6$	eutectic	(Fe,Mn,Ni)-FCC+(AlNi)-B2	[42]
34	$Fe_{36}Ni_{18}Mn_{33}Al_{13}$	eutectic	(Fe,Mn,Ni)-FCC+(AlNi)-B2	[43]
35	$Fe_{30}Ni_{20}Mn_{35}Al_{15}$	eutectic	(Fe,Mn,Ni)-FCC+(AlNi)-B2	[44]
36	$AlCrFeNiTi_{0.25}$	eutectic	(Fe,Cr)-BCC+(AlNi)-B2	[45]
37	$Zr_{0.6}CoCrFeNi_{2.0}$	eutectic	FCC+Ni_7Zr_2	[46]
38	$Nb_{0.74}CoCrFeNi_{2.0}$	eutectic	FCC+$(Co,Ni)_2Nb$	[46]
39	$Hf_{0.55}CoCrFeNi_{2.0}$	eutectic	FCC+Ni_7Hf_2	[46]
40	$Ta_{0.65}CoCrFeNi_{2.0}$	eutectic	FCC+$(Co,Ni)_2Ta$	[46]
41	$CoCrFeNiNb_{0.45}$	eutectic	FCC + Laves C15	[47,49]
42	$CoCrFeNiTa_{0.4}$	eutectic	FCC + Laves C15	[48,49]
43	$CoCrFeNiZr_{0.55}$	eutectic	FCC + Laves C14	[49]
44	$CoCrFeNiHf_{0.4}$	eutectic	FCC + Laves C14	[49]
45	$Al_{17}Co_{14.3}Cr_{14.3}Fe_{14.3}Ni_{40.1}$	eutectic	$L1_2$+B2	[50]
46	$Al_{17}Co_{28.6}Cr_{14.3}Fe_{14.3}Ni_{25.8}$	eutectic	FCC+B2	[50]
47	$Al_{17}Co_{14.3}Cr_{14.3}Fe_{28.6}Ni_{25.8}$	eutectic	FCC+B2	[50]
...	...	...	...	...

the mixing enthalpy and binary phase diagrams. The EHEA compositions are obtained by the equal-molar ratio mixing of binary eutectic compositions. For example, the mixing enthalpies of the atomic pairs, Co-Cr, Co-Ni, Co-Fe, Cr-Ni, Cr-Fe, and Fe-Ni, are close to zero, while the mixing enthalpies between Nb, Ta, Zr, Hf elements and Co, Cr, Fe, Ni elements are quite negative. Furthermore, the (Co, Cr, Fe, Ni) - (Nb, Ta, Zr, Hf) binary systems exhibit eutectic reactions. Therefore, (CoCrFeNi)-(Nb, Ta, Zr, Hf) elements are chosen to design EHEAs, and four new EHEA compositions, namely, $CoCrFeNiNb_{0.45}$, $CoCrFeNiTa_{0.4}$, $CoCrFeNiZr_{0.55}$, and $CoCrFeNiHf_{0.4}$ were discovered using the simple mixing method, as shown in Fig. 2.

3.3. The pseudo binary method

Jin et al. [50] proposed a pseudo binary method to design EHEAs, which are composed of FCC/B2 eutectic structures. In their method, the EHEA is regarded as an FCC-NiAl intermetallic compound (B2) pseudo binary alloy, and the FCC phase and intermetallic compound phase should be stable enough, compared to the pure component. Based on this strategy, three FCC-structured $CoCrFeNi_2$, $Co_2CrFeNi$, and $CoCrFe_2Ni$ were taken as the FCC component, and NiAl was taken as the other component in the pseudo binary alloys. Several new EHEA compositions, such as $Al_{17}Co_{14.3}Cr_{14.3}Fe_{14.3}Ni_{40.1}$, $Al_{17}Co_{28.6}Cr_{14.3}Fe_{14.3}Ni_{25.8}$, $Al_{17}Co_{14.3}Cr_{14.3}Fe_{28.6}Ni_{25.8}$, were located using this method.

3.4. The semi-quantitative method based on CALPHAD

Beyond empirical rules, a semi-quantitative method based on CALPHAD was also developed to locate eutectic alloys in the multi-principal-element system. Although the database of HEAs are still lacking, several pioneer works demonstrated that the CALPHAD simulation greatly accelerates the design of EHEAs. The first trial was found in the work by He et al. [34]. Binary phase diagrams are firstly reviewed to search for eutectic alloys, and they form the subset binary systems that are required to form a EHEA system. Based on this assumption, the compositional space of the EHEAs are quickly narrowed down by screening existing binary phase diagrams. The CALPHAD simulations are applied to further pinpoint the EHEA compositions. A typical example is the $CoCrFeNiNb_x$ EHEA system. The five constituent elements are chosen because

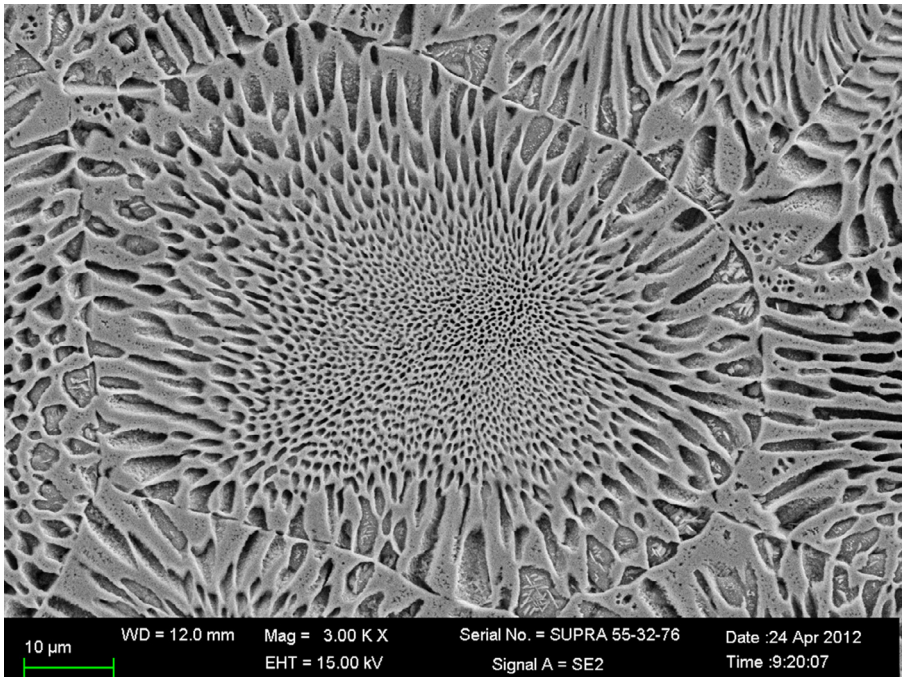

Fig. 1. The microstructure of $AlCrFeNiMo_{0.2}$ EHEA [22].

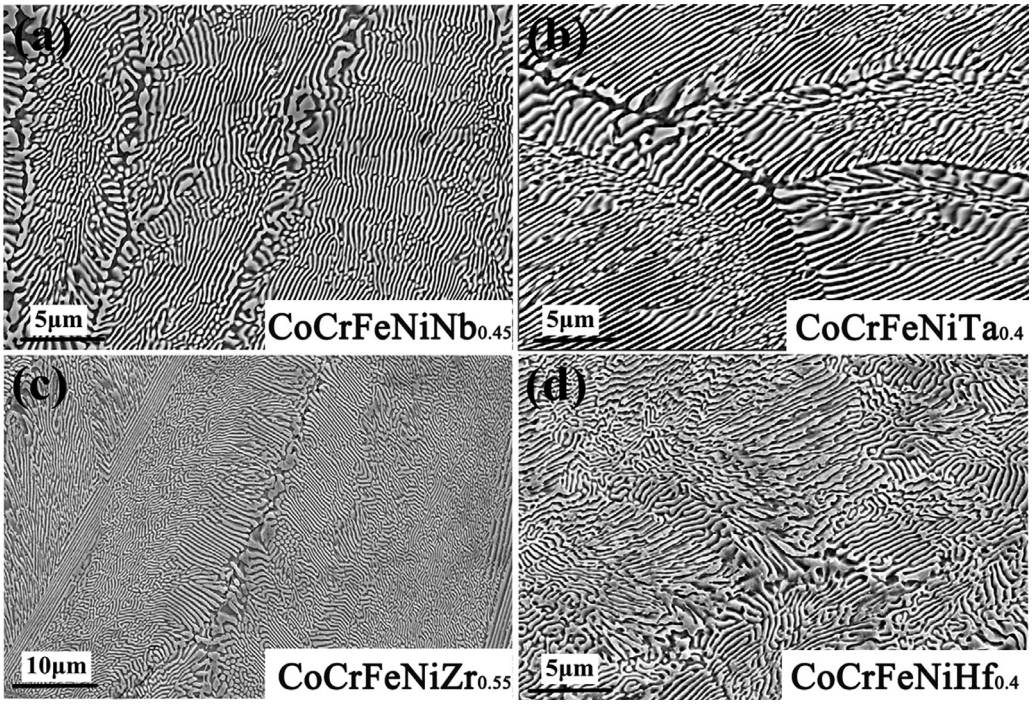

Fig. 2. Microstructure of the CoCrFeNi-M (M=Nb, Ta, Zr, Hf) EHEAs: (a) $CoCrFeNiNb_{0.45}$, (b) $CoCrFeNiTa_{0.4}$, (c) $CoCrFeNiZr_{0.55}$, and (d) $CoCrFeNiHf_{0.4}$ [49].

the binary phase diagrams of Ni-Nb, Co-Nb, Cr-Nb, and Fe-Nb systems all exhibit eutectic points at the positions of 14 atomic percent (at. %) Nb. Since the CoCrFeNi HEA possesses single-phase solid solutions at high temperatures [52,53], it is reasonable to locate the EHEAs composition in a pseudo-binary (CoCrFeNi)-Nb_x phase diagram. The validity of the method was successfully proved by the microstructures of the $CoCrFeNiNb_x$ EHEAs. Following this CALPHAD-assisted design approach, $CoCrFeNiTa_{0.43}$, $AlCoCrFeNi_3$, $AlCo_2CrFeNi_2$, and $AlCoCrFe_2Ni_2$, $CoCrFeNiZr_{0.5}$ EHEAs were developed [50,54,55].

With the development of the CALPAHD-assisted alloy design idea, a more general grouping strategy based on the intrinsic formation mechanism of the lamellar structures was proposed [56]. The emphasis of the grouping strategy is on the solidification behaviors of the eutectic alloys. During solidification, components of an EHEA system tend to separate into two groups, and each of which forms one phase when the temperature decreases to the solid line. Accordingly, a eutectic structure can be expected in a new multi-component alloy system if the designed components can be divided into two groups. The standard deviation of the dis-

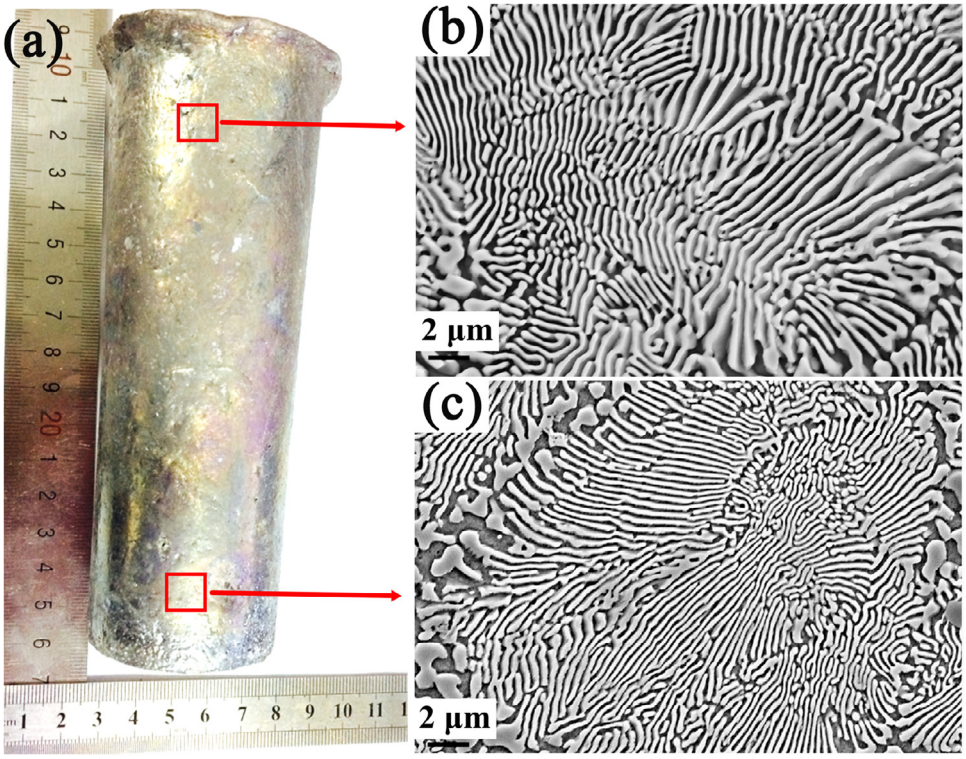

Fig. 3. (a) Appearance of the bulk $CoCrFeNiNb_{0.45}$ EHEA ingot. (b) The microstructure observed in the upper part of the ingot. (c) The microstructure observed in the bottom part of the ingot [23].

tribution of mixing enthalpies of binary systems was suggested to characterize the thermodynamic features of alloys systems that can be divided into two groups. This grouping strategy was successively supported by the discovery of new EHEAs, $Ni_2CoCrFeNb_{0.74}$, $CoCrFeNiTa_{0.43}$, $Ni_2CoCrFeHf_{0.55}$, and $CoCrFeNiZr_{0.5}$.

3.5. The machine-learning method

There are several composition variables in a multicomponent system. Based on the phase rule, there should form a series of eutectics. It is a great challenge to determine all the eutectic compositions in each alloy system. The machine-learning method has been applied to predict the eutectics in multi-principal-element alloys [57]. In the Al-Co-Cr-Fe-Ni system, a database containing the alloy compositions and phase constitutions of 321 alloys was built up using the literature results and CALPHAD calculations. The artificial neural network model was then trained to predict a large number of near-eutectic compositions. By analyzing the predicted compositions, the association between different elements and eutectic formation was established, as shown in Fig. 6. It was found that Al is the critical element for the eutectic formation, the content of which should be between 15 to 20 at.%. Cr is the strongly associated element with Al, i.e., there is a corresponding eutectic content range for Cr when fixing the Al content. As for the miscible Ni, Co, and Fe elements, their contents can be estimated using the average valence electron concentration. This research in Ref. [57] not only revealed the eutectic formation in the Al-Co-Cr-Fe-Ni system, but also provided a three-step design method to locate EHEAs in multicomponent systems: 1) divide the elements into critical elements, strongly associated elements, and miscible elements by machine learning; 2) select the combinations of critical and strongly associated elements; and 3) determine the contents of miscible elements. In the future, the machine learning method is expected to be a promising method to develop abundant EHEAs with the development of databases.

4. Future trends

4.1. New alloy systems

Metallic casting parts are widely used in various industrial fields. In all cast alloys, eutectic alloys are the most widely used because of their excellent castability. EHEAs have the advantages of both HEAs and eutectic alloys, which brings the hope for the large-scale and extensive industrial application of HEAs. Most of the reported EHEAs can be divided into two categories according to their microstructures. The first kind of EHEAs is composed of two hard phases, such as BCC/B2 phases [22,41,45]. They cannot be applied in a load-bearing structure especially when cyclic fatigue exists, but could be used as functional materials. The second kind of EHEAs is composed of a hard phase and a soft phase, such as FCC+BCC (B2) or FCC/intermetallic phases, which generally exhibits excellent mechanical properties and can be used for load-bearing structures. The second kind of EHEAs includes $AlCoCrFeNi_{2.1}$ [10], $Al_{0.7}CoFeNi_2$ [25], $AlCrFeNi_3$ [12], $Co_{30}Cr_{10}Fe_{10}Al_{18}Ni_{32}$ [26], $CrFeNi_{2.2}Al_{0.8}$ [18], $Al_{16}Co_{41}Cr_{15}Fe_{10}Ni_{18}$ [27], $Ni_{30}Co_{30}Cr_{10}Fe_{10}Al_{18}W_2$ [19], $Fe_{20}Co_{20}Ni_{41}Al_{19}$ [17], $Fe_{28.2}Ni_{18.8}Mn_{32.9}Al_{14.1}Cr_6$ [42], $Fe_{36}Ni_{18}Mn_{33}Al_{13}$ [43], $Fe_{30}Ni_{20}Mn_{35}Al_{15}$ [44], and $Ni_{24}Co_{36}Fe_{10}Cr_{10}Al_{18}W_2$ [57], all displaying the tensile fracture strength $\geq$ ~ 1,000 MPa and good tensile ductility with a uniform elongation of 5~30% in the cast state. The second kind of EHEAs has wide application scopes and great potential in industrial applications. Much of the current work in the field of EHEAs is focused on the alloy design or optimization of the second kind of EHEAs. Since many EHEAs contain expensive elements, such as Co, how to remove the expensive elements

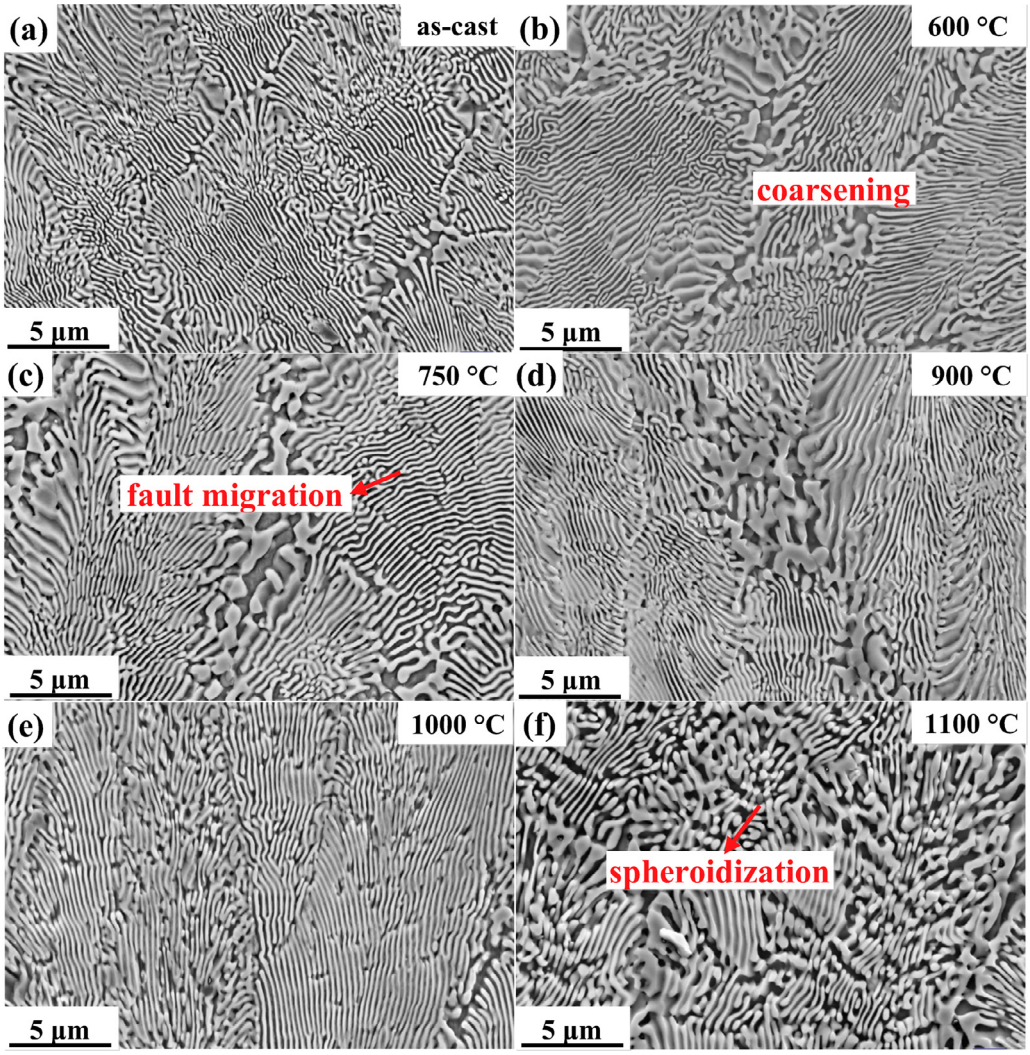

Fig. 4. Microstructures of the as-cast and as-annealed $CoCrFeNiNb_{0.45}$ HEAs: (a) as-cast, and after annealing for 4 h at various temperatures (b) 600°C, (c) 750°C, (d) 900°C, (e) 1,000°C, and (f) 1,100°C [23].

while still maintaining the excellent performance of EHEAs is the focus of the future work.

4.2. New processing routes

EHEAs are easy to be synthesized because of their excellent castability. Most EHEAs are prepared by conventional melting methods, such as arc melting or electromagnetic induction melting [10-23,58]. Despite the simplicity of the melting process, EHEAs generally exhibit a fine and uniform lamellar microstructure. Ding et al. reported that EHEA prepared using the powder produced by the gas-atomization method also possess excellent mechanical properties and good corrosion resistance properties [59]. Their results indicated that EHEAs are not only suitable for casting, but also suitable for powder metallurgy and additive manufacturing. Chen et al. and Wang et al. studied the effects of directional solidification on the microstructures and mechanical properties of EHEAs [60,61]. Their results suggest that the mechanical properties of EHEAs could be further improved under directional-solidification conditions, especially the tensile ductility, for example the uniform tensile elongation of $AlCoCrFeNi_{2.1}$ can be improved to $\geq$ 35%. The uniform elongation was greatly increased because the directional solidification significantly reduced casting defects. Bhattacharjee et al. [62-64], Phanikumar et al. [65], Tsuji et al. [66,67], and Mishra et al. [68,69] studied the effects of thermomechanical treatments on mechanical properties of EHEAs. Their works show that the thermo-mechanically treated $AlCoCrFeNi_{2.1}$ EHEAs can have the tensile fracture strength up to 1,950 MPa, tensile yield strength up to 1,650 MPa, and still have the tensile elongation of more than 5%. It clearly suggests that although the mechanical properties of EHEAs have been excellent, there is still much room for improvement via subsequent processing. Therefore, new processing routes with further improvement in mechanical properties could increase the industrial application potential of EHEAs.

5. Potential applications

The EHEAs can be excellent structural and functional materials, with great potential in industrial applications [70,71]. EHEAs containing Al and Cr elements have excellent seawater corrosion resistance and high-temperature oxidation resistance. The prototype $AlCoCrFeNi_{2.1}$ EHEA with high concentrations of Al and Cr shows seawater corrosion resistance beyond all copper alloys that are used as propeller materials currently in service, and it can also be expected to possess good oxidation resistance at high temperatures [11]. At the same time, the $AlCoCrFeNi_{2.1}$ EHEA has also been shown to be useful over a wide temperature spectrum, and their

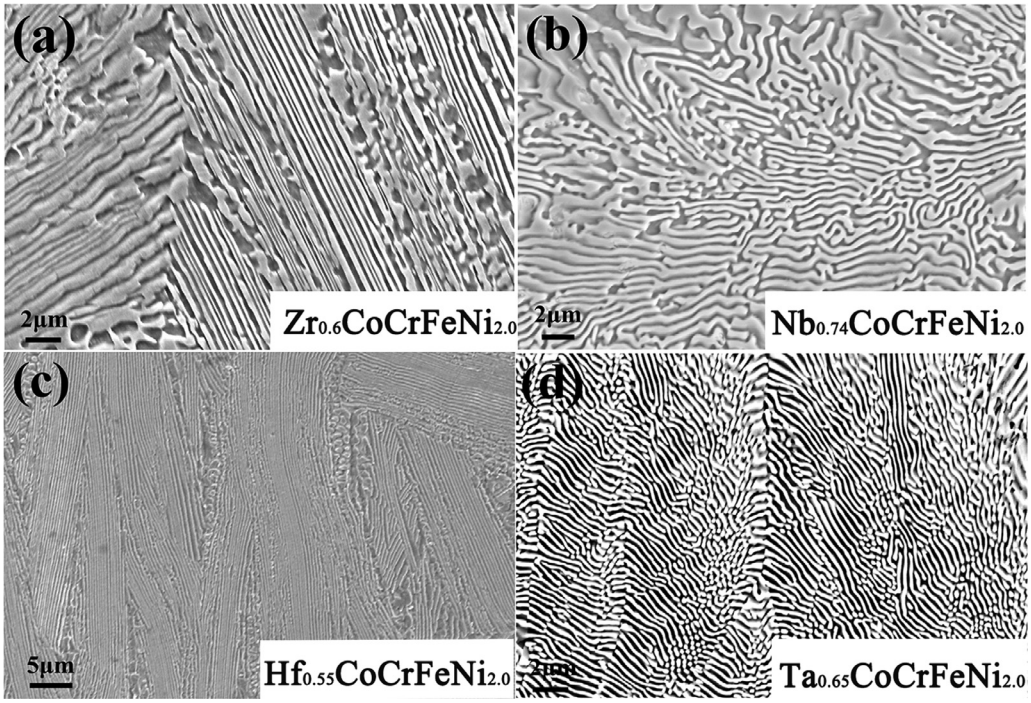

Fig. 5. The microstructure of designed $CoCrFeNi_{2.0}$-M (M=Zr, Nb, Hf, Ta) EHEAs by the current authors: (a) $Zr_{0.6}CoCrFeNi_{2.0}$, (b) $Nb_{0.74}CoCrFeNi_{2.0}$, (c) $Hf_{0.55}CoCrFeNi_{2.0}$, (d) $Ta_{0.65}CoCrFeNi_{2.0}$ [46].

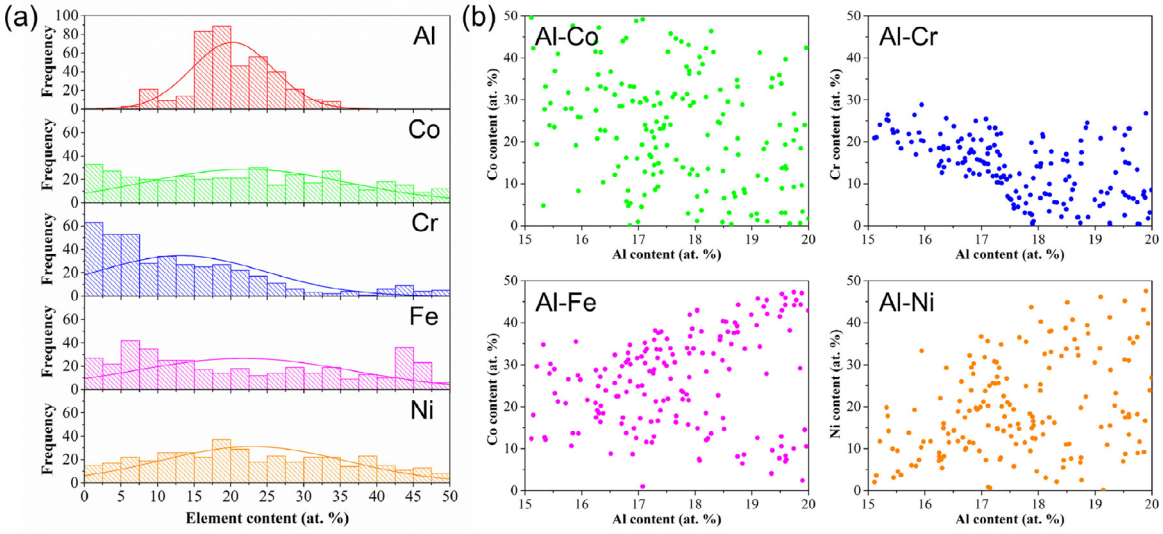

Fig. 6. Statistics on the 400 predicted near-eutectic compositions. (a) Content distributions of every single element. (b) Maps showing the contents of Co, Cr, Fe, Ni corresponding to the Al content [57].

excellent mechanical properties were demonstrated from 77K to as high as 1,000K. EHEAs with excellent mechanical properties and seawater corrosion resistance can be widely applied in propeller for ice-breakers instead of copper alloys and stainless steels, and also in ships, pipelines, valves, motor housing, acid pump components, offshore oil platform, and complex structural castings requiring both excellent mechanical properties and corrosion resistance.

Another promising application direction for EHEAs is as a functional material. Recently, Tsai et al. reported some EHEAs have good damping properties and can be used as shock absorbers [20]. Also, if the lamellar spacing of alloys is about tens of nanometers, with one being the hard magnetic phase and the other being the soft magnetic phase, a giant magnetoresistance effect would occur. With designed structures and properties, EHEAs could be revolutionary metallic materials.

6. Conclusions

The development history, the unique solidification microstructure, and the alloy-design strategies of EHEAs are briefly reviewed here. EHEAs possess the advantages of both high entropy alloys and eutectic alloys, and the concept of EHEAs can be readily adapted to the large-scale industrial production of ingots with fine and uniform lamellar microstructures. EHEAs can be excellent structural materials exhibiting simultaneously high strength and great ductility. With better cost control, EHEAs could well be the

first used alloys in large-scale industrial applications in the domain of HEAs.

Declaration of Competing Interest

The authors declare that they have no known competing financial interests or personal relationships that could have appeared to influence the work reported in this paper.

Acknowledgments

This work was supported by the National Natural Science Foundation of China (Nos. 51822402, 51671044, and 51901116), and the National Key Research and Development Program of China (No.2019YFA0209901), the National MCF Energy R&D Program (project No. 2018YFE0312400), the Fundamental Research Funds for the Central Universities (DUT16ZD206), and the Liao Ning Revitalization Talents Program (XLYC 1807047). PKL very much appreciates the support of the U.S. Army Research Office Project (W911NF-13-1-0438 and W911NF-19-2-0049) with the program managers, Drs. M. P. Bakas, S. N. Mathaudhu, and D. M. Stepp. PKL thanks the support from the National Science Foundation (DMR-1611180 and 1809640) with the program directors, Drs. J. Yang, J., G. Shiflet, and D. Farkas.

References

[1] J.W. Yeh, S.K. Chen, S.J. Lin, J.Y. Gan, T.S. Chin, T.T. Shun, C.H. Tsau, S.Y. Chang, Adv. Eng. Mater. 6 (2004) 299–303.
[2] B. Cantor, I.T.H. Chang, P. Knight, A.J.B. Vincent, Mater. Sci. Eng. A 375-377 (2004) 213–218.
[3] B. Gludovatz, A. Hohenwarter, D. Catoor, E.H. Chang, E.P. George, R.O. Ritchie, Science 345 (2014) 1153–1158.
[4] Y. Zhang, T.T. Zuo, Z. Tang, M.C. Gao, K.A. Dahmen, P.K. Liaw, Z.P. Lu, Prog. Mater. Sci. 61 (2014) 1–93.
[5] Z.M. Li, K.G. Pradeep, Y. Deng, D. Raabe, C.C. Tasan, Nature 534 (2016) 17981.
[6] Z. Lei, X. Liu, Y. Wu, H. Wang, S.H. Jiang, S.D. Wang, X.D. Hui, Y.D. Wu, B. Gault, P. Kontis, D. Raabe, L. Gu, Q.H. Zhang, H.W. Chen, H.T. Wang, J.B. Liu, K. An, Q.S. Zeng, T.G. Nieh, Z.P. Lu, Nature 563 (2018) 546–550.
[7] B.S. Murty, J.W. Yeh, S. Ranganathan, High Entropy Alloys, Butterworth-Heinemann, London, 2014.
[8] M.C. Gao, J.W. Yeh, P.K. Liaw, Y. Zhang, High-Entropy Alloys: Fundamentals and Applications, Springer Verlag, New York, 2016.
[9] M.E. Glicksman, Principles of Solidification: An Introduction to Modern Casting and Crystal Growth Concepts, Springer Verlag, New York, 2010.
[10] Y.P. Lu, Y. Dong, S. Guo, L. Jiang, H.J. Kang, T.M. Wang, B. Wen, Z.J. Wang, J.C. Jie, Z.Q. Cao, H.H. Ruan, T.J. Li, Sci. Rep. 4 (2014) 6200.
[11] Y.P. Lu, X.Z. Gao, L. Jiang, Z.N. Chen, T.M. Wang, J.C. Jie, H.J. Kang, Y.B. Zhang, S. Guo, H.H. Ruan, Y.H. Zhao, Z.Q. Cao, T.J. Li, Acta. Mater. 124 (2017) 143–150.
[12] Y. Dong, Z.Q. Yao, X. Huang, F.M. Du, C.Q. Li, A.F. Chen, F. Wu, Y.Q. Cheng, Z.R. Zhang, J. Alloys. Compd. 823 (2020) 153886.
[13] Y.F. Liao, I. Baker, J. Mater. Sci. 46 (2011) 2009–2017.
[14] Y. Dong, Y.P. Lu, Arab. J. Sci. Eng. 44 (2019) 803–808.
[15] Z.G. Zhu, K.H. Ma, Q. Wang, C.H. Shek, Intermetallics 79 (2016) 1–11.
[16] X. Jin, Y.X. Liang, J. Bi, B.S. Li, Materialia 10 (2020) 100639.
[17] X. Jin, Y. Zhou, L. Zhang, X.Y. Du, B.S. Li, Mater. Lett. 216 (2018) 144–146.
[18] X. Jin, J. Bi, L. Zhang, Y. Zhou, X.Y. Du, Y.X. Liang, B.S. Li, J. Alloys. Compd. 770 (2019) 655–661.
[19] Q.F. Wu, Z.J. Wang, T. Zheng, D. Chen, Z.S. Yang, J.J. Li, J.J. Kai, J.C. Wang, Mater. Lett. 253 (2019) 268–271.
[20] L.F. Lin, C.W. Tsai. Philos. Mag. Lett. 10.1080/09500839.2019.1660819.
[21] I. Baker, M. Wu, Z.W. Wang, Mater. Charact. 147 (2019) 545–557.
[22] Y. Dong, Y.P. Lu, J.R. Kong, J.J. Zhang, T.J. Li, J. Alloys. Compd. 573 (2013) 96–101.
[23] H. Jiang, D.X. Qiao, Y.P. Lu, Z. Ren, Z.Q. Cao, T.M. Wang, T.J. Li, Scr. Mater. 165 (2019) 145–149.
[24] Y. Dong, L. Jiang, Z.Y. Tang, Y.P. Lu, T.J. Li, J. Mater. Eng. Perform. 24 (2015) 4475–4481.
[25] S. Guo, C. Ng, C.T. Liu, J. Alloys Compd. 557 (2013) 77–81.
[26] Z.S. Yang, Z.J. Wang, Q.F. Wu, T. Zheng, P. Zhao, J.K. Zhao, J.Y. Chen, Appl. Phys. A 125 (2019) 208.
[27] A. Shafiei, S. Rajabi, Appl. Phys. A 125 (2019) 783.
[28] S. Vrtnik, S. Guo, S. Sheikh, A. Jelen, P. Kozelj, J. Luzar, A. Kocjan, Z. Jalicic, A. Meden, H. Guim, H.J. Kim, J. Dolinsek, Intermetallics 93 (2018) 122–133.
[29] W.Y. Huo, H. Zhou, F. Fang, X.F. Zhou, Z.H. Xie, J.Q. Jiang, J. Alloys Compd. 735 (2018) 897–904.
[30] Y.M. Tan, J.S. Li, J. Wang, M. Kolbe, H.C. Kou, J. Alloys Compd. 731 (2018) 600–611.
[31] R. Jain, M.R. Rahul, S. Jain, S. Samal, V. Kumar, Trans. Indian. Inst. Met. 71 (11) (2018) 2795–2799.
[32] Z.Y. Ding, Q.F. He, Q. Wang, Y. Yang, Inter. J .Plast. 106 (2018) 57–72.
[33] M.R. Rahul, G. Phanikumar, Metall. Mater. Trans. A 50A (2019) 2594–2598.
[34] F. He, Z.J. Wang, P. Cheng, Q. Wang, J.J. Li, Y.Y. Dang, J.C. Wang, C.T. Liu, J. Alloys Compd. 656 (2016) 284–289.
[35] Ł. Rogal, J. Morgiel, Z. Świątek, F. Czerwiński, Mater. Sci. Eng. A 651 (2016) 590–597.
[36] L. Jiang, Y.P. Lu, Y. Dong, T.M. Wang, Z.Q. Cao, T.J. Li, Appl. Phys. A. 119 (2015) 291–297.
[37] L. Jiang, Z.Q. Cao, J.C. Jie, J.J. Zhang, Y.P. Lu, T.M. Wang, T.J. Li, J. Alloys Compd. 649 (2015) 585–590.
[38] H. Jiang, H.Z. Zhang, T.D. Huang, Y.P. Lu, T.M. Wang, T.J. Li, Mater. Des. 109 (2016) 539–546.
[39] D.J. Liu, P.F. Yu, G. Li, P.K. Liaw, R.P. Liu, Mater. Sci. Eng. A 724 (2018) 283–288.
[40] Y. Guo, L. Liu, Y. Zhang, J.G. Qi, B. Wang, Z.F. Zhao, J. Shang, J. Xiang, J. Mater. Res. 33 (19) (2018) 3258–3265.
[41] X. Chen, J.Q. Qi, Y.W. Sui, Y.Z. He, F.X. Wei, Q.K. Meng, Z. Sun, Mater. Sci. Eng. A 681 (2017) 25–31.
[42] I. Baker, F.L. Meng, M. Wu, A. Brandenberg, J. Alloys Compd. 656 (2016) 458–464.
[43] Z.W. Wang, M. Wu, Z.H. Cai, S. Chen, I. Baker, Intermetallics 75 (2016) 79–87.
[44] F.L. Meng, I. Baker, J. Alloys Compd. 645 (2015) 376–381.
[45] S. Liu, M.C. Gao, P.K. Liaw, Y. Zhang, J. Alloys Compd. 619 (2015) 610–615.
[46] Y.P. Lu, H. Jiang, S. Guo, T.M. Wang, Z.Q. Cao, T.J. Li, Intermetallics 91 (2017) 124–128.
[47] H. Jiang, K.M. Han, D.X. Qiao, Y.P. Lu, Z.Q. Cao, T.J. Li, Mater. Chem. Phys. 210 (2018) 43–48.
[48] H. Jiang, L. Jiang, D.X. Qiao, Y.P. Lu, T.M. Wang, Z.Q. Cao, T.J. Li, J. Mater. Sci. Tech. 33 (2017) 712–717.
[49] H. Jiang, K. Han, X. Gao, Y. Lu, Z. Cao, M.C. Gao, J.A. Hawk, T. Li, Mater. Des. 142 (2018) 101–105.
[50] X. Jin, Y. Zhou, L. Zhang, X.Y. Du, B.S. Li, Mater. Des. 143 (2018) 49–55.
[51] Z.Y. Ding, Q.F. He, Y. Yang, Sci. China-Tech. Sci. 61 (2018) 159–167.
[52] F. He, Z. Wang, Q. Wu, J. Li, J. Wang, C.T. Liu, Scr. Mater. 126 (2017) 15–19.
[53] F. He, Z. Wang, Q. Wu, S. Niu, J. Li, J. Wang, C.T. Liu, Scr. Mater. 131 (2017) 42–46.
[54] C. Ai, F. He, M. Guo, J. Zhou, Z. Wang, Z. Yuan, Y. Guo, Y. Liu, L. Liu, J. Alloys Compd. 735 (2018) 2653–2662.
[55] W. Huo, H. Zhou, F. Fang, Z. Xie, J. Jiang, Mater Des. 134 (2017) 226–233.
[56] F. He, Z. Wang, C. Ai, J. Li, J. Wang, J.J. Kai, Mater. Chem. Phys. 221 (2019) 138–143.
[57] Q.F. Wu, Z.J. Wang, X.B Hu, T. Zheng, Z.S. Yang, F. He, J.J. Li, J.C. Wang, Acta. Mater. 182 (2020) 278–286.
[58] Y. Dong, Y.P. Lu, J. Mater. Eng. Perform. 27 (2018) 109–115.
[59] P.P. Ding, A. Mao, X. Zhang, X. Jin, B. Wang, M. Liu, X.L. Gu, J. Alloys Compd. 721 (2017) 609–614.
[60] H.T. Zheng, R.R. Chen, G. Qin, X.Z. Li, Y.Q. Su, H.S. Ding, J.J. Guo, H.Z. Fu, Intermetallics 113 (2019) 106569.
[61] L. Wang, C.L. Yao, J. Shen, Y.P. Zhang, T. Wang, Y.H. Ge, L.H. Gao, G.J. Zhang, Intermetallics 118 (2020) 106681.
[62] I.S. Wani, T. Bhattacharjee, S. Sheikh, P.P. Bhattacharjee, S. Guo, N. Tsuji, Mater. Sci. Eng. A 675 (2016) 99–109.
[63] A. Patel, I. Wani, S.R. Reddy, S. Narayanaswamy, A. Lozinko, R. Saha, S. Guo, P.P. Bhattacharjee, Intermetallics 97 (2018) 12–21.
[64] I.S. Wani, T. Bhattacharjee, S. Sheikh, I.T. Clark, M.H. Park, T. Okawa, S. Guo, P.P. Bhattacharjee, N. Tsuji, Intermetallics 84 (2017) 42–51.
[65] M.R. Rahul, S. Samal, S. Venugopal, G. Phanikumar, J. Alloys Compd. 749 (2018) 1115–1127.
[66] T. Bhattacharjee, I.S. Wani, S. Sheikh, I.T. Clark, T. Okawa, S. Guo, P.P. Bhattacharjee, N. Tsuji, Sci. Rep. 8 (2018) 3276.
[67] T. Bhattacharjee, R.X. Zheng, Y. Chong, S. Sheikh, S. Guo, I.T. Clark, T. Okawa, I.S. Wani, P.P. Bhattacharjee, A. Shibata, N. Tsuji, Mater. Chem. Phys. 210 (2018) 207–212.
[68] T.H. Wang, M. Komarasamy, S. Shukla, R.S. Mishra, J. Alloys Compd. 766 (2018) 312–317.
[69] S. Shukla, T.H. Wang, S. Cotton, R.S. Mishra, Scripta Mater. 156 (2018) 105–109.
[70] L.L. Han, X.D. Xu, L. Wang, F. Pyczak, R. Zhou, Y. Liu, Mater. Res. Lett. 7 (11) (2019) 460–466.
[71] Y. Dong, L. Jiang, H. Jiang, Y.P. Lu, T.M. Wang, T.J. Li, Mater. Des. 82 (2015) 91–97.